Solar Energy Materials & Solar Cells 121 (2014) 61–68

Contents lists available at ScienceDirect

Solar Energy Materials & Solar Cells

journal homepage: www.elsevier.com/locate/solmat

Influence of acetylene-linked π-spacers on triphenylamine–fluorene dye sensitized solar cells performance

Alexis Tigreros [a], Vivek Dhas [b], Alejandro Ortiz [a], Braulio Insuasty [a,*], Nazario Martín [c], Luis Echegoyen [b,*]

[a] Grupo de Investigación de Compuestos Heterocíclicos, Departamento de Química, Universidad del Valle, A.A. 25360 Cali, Colombia
[b] Department of Chemistry, University of Texas at El Paso, El Paso, TX 79968-0519, United States
[c] Departamento de Química Orgánica, Facultad de Química, Universidad Complutense, 28040 Madrid, Spain

ARTICLE INFO

Article history:
Received 21 May 2013
Received in revised form
26 October 2013
Accepted 28 October 2013
Available online 21 November 2013

Keywords:
Ethynilfluorene
Dye sensitized solar cells
Acetylene linkage

ABSTRACT

Four new organic dyes, **1–4,** containing triphenylamine (TPA) donors connected through different acetylene linkages to fluorene bridges and cyanoacrylic acid acceptors were designed and synthetized for photoconversion in dye sensitized solar cells (DSSCs). Their absorption spectra, electrochemical and photovoltaic properties were investigated. Shortening the bridge between the TPA moiety and the anchoring group leads to a dramatic increase in the overall photoconversion efficiency (**1** > **3** > **4** > **2**).

1. Introduction

The conversion of solar energy directly into electricity is one of the most attractive renewable energy sources that could help replace fossil fuels and control global warming [1]. Since the first report in 1991 by O'regan and Grätzel, dye sensitized solar cells (DSSCs) have emerged as one of the most promising low-cost alternative for renewable generation of electricity [2].

In DSSCs the sensitizer is the crucial component, which absorbs the light and injects electrons into the conduction band of the semiconductor [3,4]. The optimization of this component has resulted in the development of new compounds to improve the absorption, morphology and stability. Ruthenium [5], triarylamines [6], squarines [7], thiophenes [8,9], porphyrins [10,11] and π-extended tetrathiafulvalenes (exTTFs) [12] have been incorporated and tested with promising results. In the past decades, there has been a growing interest in finding new sensitizers that are easy to prepare, exhibit high efficiency in solar energy conversion and can be prepared from easily available materials in order to avoid the high cost of the most efficient dyes, which contain ruthenium(II) [13].

Fluorene is an electron rich moiety with a high molar extinction coefficient, relatively low cost, is easy to functionalize by simple chemical modifications [14,15] and possesses outstanding electron transfer properties [16], therefore it is potentially useful for photovoltaic applications [17]. Actually, fluorene is present in numerous dyes which exhibit efficiencies ranging from moderate to excellent in DSSCs [18–21].

On the other hand, the rod-like shape of the ethynyl groups, where conjugation occurs through a cylindrical electronic structure [22], along with its synthetic availability via cross-coupling reactions and the absence of photostability problems compared to vinyl connectors [23], make this group a very attractive link in materials science, compared with other π-connecting groups.

Based on these observations, a series of donor–spacer–acceptor molecules **1–4** (Fig. 1) having triphenylamine (TPA) donors, fluorene bridges, and cyanoacrylic acid acceptors were synthetized and studied as sensitizers in DSSCs. Taking advantage of the high synthetic versatility of the ethynyl functional group to connect the donor and spacer moieties via Sonogashira and Glaser coupling reactions, along with the well known acetylide platinum chemistry [24–27], we studied the influence of the π-connection through different acetylene linkages on the photoconversion efficiencies. A simple acetylene group (**1**) is a better π-connector when compared with the other π-connectors studied, namely 2,7-bisethynyl-9,9-dioctylfluorene (**2**), 1,3-butadiyne (**3**) and platinum acetylide complex (**4**), despite the fact that these have much higher optical densities.

2. Results and discussion

2.1. Syntheses

The synthetic routes followed to prepare compounds **1–4** are presented in Schemes 1 and 2. The starting compounds

* Corresponding authors. Tel.: +1 864 656 6112; fax: +1 864 656 6613.
E-mail address: echegoyen@utep.edu (L. Echegoyen).

0927-0248/$ - see front matter © 2013 Elsevier B.V. All rights reserved.
http://dx.doi.org/10.1016/j.solmat.2013.10.035

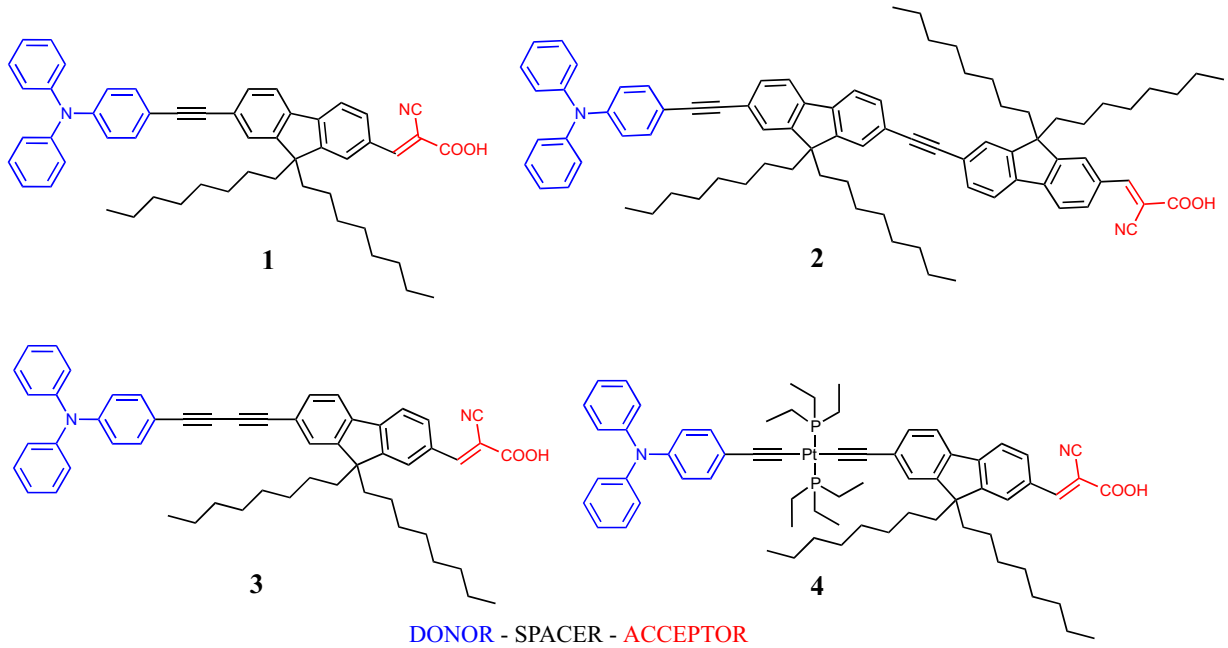

Fig. 1. Molecular structures of the new sensitizers **1–4.**

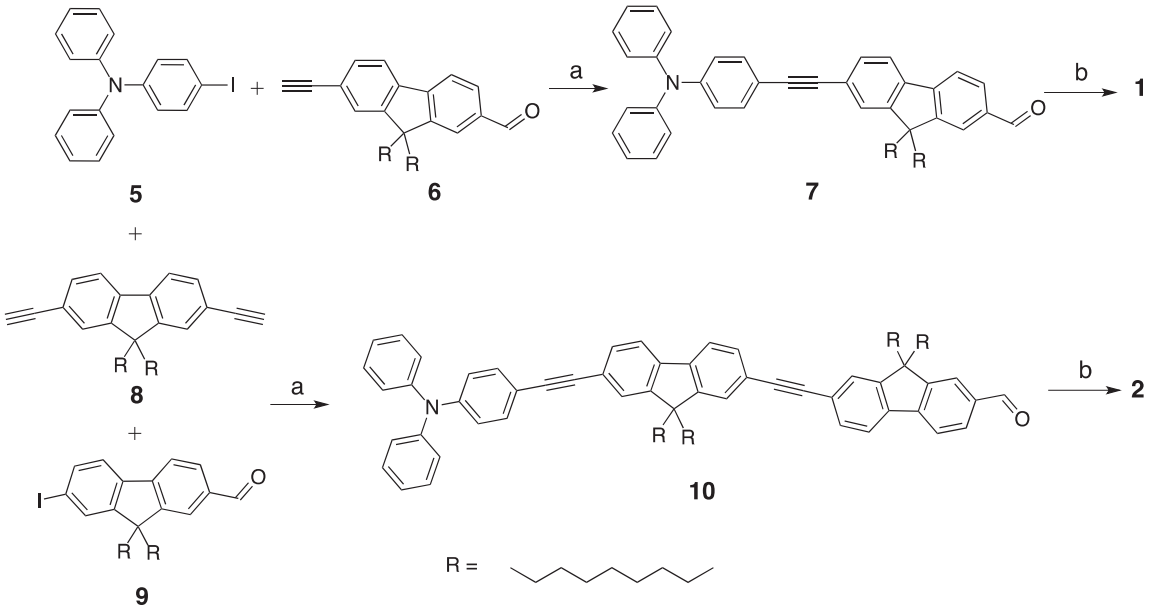

Scheme 1. Synthetic routes for **1** and **2**. (a) $Pd_2(dba)_3$, $AsPh_3$, THF, TEA: (b) AcOH, $AcNH_4$, $CNCH_2COOH$..

7-ethynyl-9,9-dioctyl-9*H*-fluorene-2-carbaldehyde **6**, 7-iodo-9,9-dioctyl-9*H*-fluorene-2-carbaldehyde **9** and 4-ethynyl-*N*,*N*-diphenylaniline **12** were prepared according to reported procedures and the analytical data are presented in the supporting information [28,29]. A Sonogashira cross-coupling reaction was used for the synthesis of intermediates **7** and **10**, and aldehyde **13** was synthesized using a Glaser cross-coupling reaction in toluene and triethylamine. Starting from the corresponding aldehyde derivatives **6**, **7**, **10** or **13**, and cyanoacetic acid in the presence of ammonium acetate and acetic acid as solvent, 2-cyano-3-(7-ethynyl-9,9-dioctyl-9*H*-fluoren-2-yl)acrylic acid **11** and the target compounds **1–3** were prepared through a Knoevenagel condensation in high yields (89–92%). Complex **4** was synthesized using a one-pot methodology via cross-coupling with *trans*-$PtCl_2(PEt_3)_2$ as the platinum source (62%).

2.2. Optical and electrochemical properties

Fig. 2 shows the UV–vis and emission spectra of dyes **1–4** in THF solution, and the data are collected in Table 1. All dyes displayed broad visible bands around 300–450 nm ($\varepsilon = 1.6–4.3 \times 10^5$ M/cm) corresponding to a superposition of the π–π^* transitions of the conjugated molecules and the intramolecular charge transfer (ICT) transition from the TPA donor to the cyanoacrylic acid acceptor. There were no notable difference in absorption bands when the linker was changed from simple ethynyl to the platinum acetylide complex, only a 6 nm shift, but the absorption coefficient was clearly affected by the introduction of additional conjugation into the system, with the exception of complex **4**, which exhibits a weak absorption coefficient when compared to **3**. However, in comparison with conventional ruthenium complexes (for example, 1.39×10^4

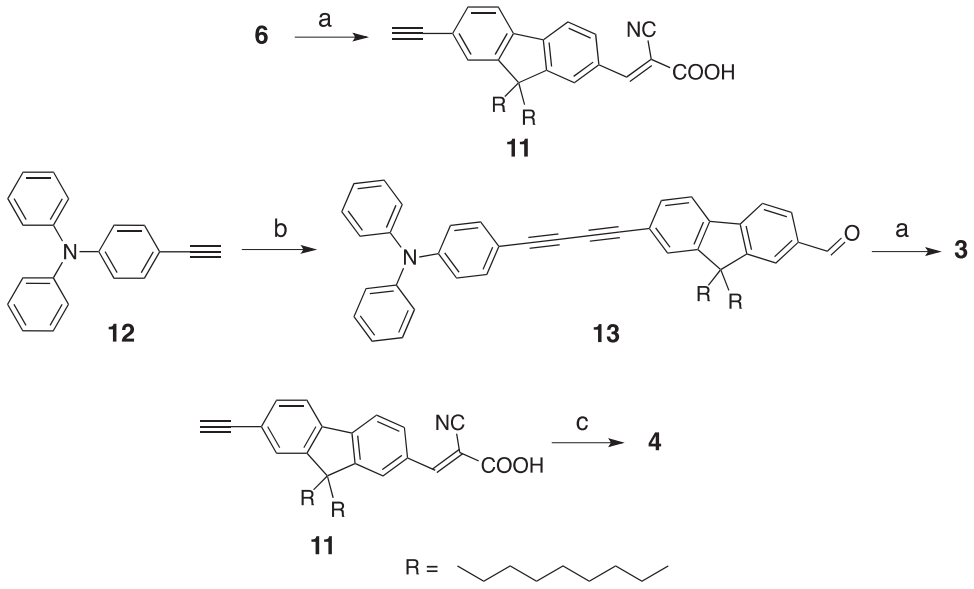

Scheme 2. Synthetic routes for **3** and **4**. (a) AcOH, $AcNH_4$, $CNCH_2COOH$; (b) **6**, $PdCl_2(PPh_3)_2$, CuI, toluene, TEA; (c) **12**, *trans*-$PtCl_2(PEt_3)_2$, DCM, TEA, CuI..

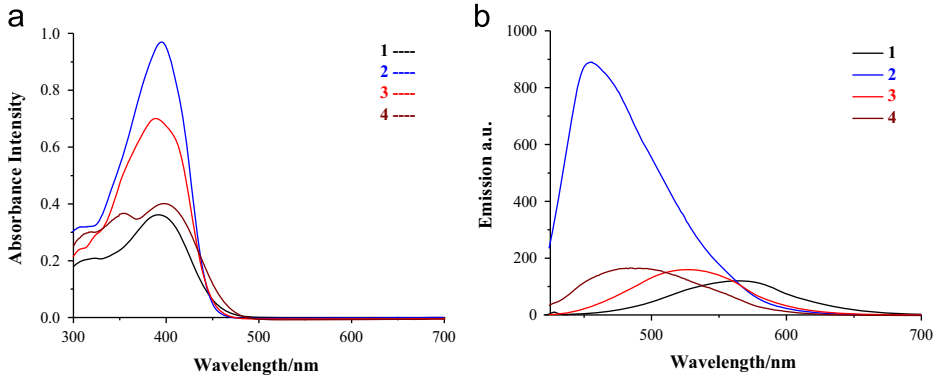

Fig. 2. Absorption spectra (a) and emission spectra of dyes **1–4** in THF (b) at 2.2×10^{-5} M.

Table 1
Optical and electrochemical properties of dyes **1–4**.

Dye	λ_{max}[a]/nm (ε/M/cm)	E_{0-0}[b]/nm (eV)	λ_{em}[c]/nm	E_{ox}[d]/V vs. NHE (HOMO)	E_{ox} shifts[e] (V)	E_{ox}*[f]/eV vs. NHE
1	393 (16,233)	507 (2.45)	545	1.18	0.27	−1.27
2	397 (43,408)	470 (2.64)	455	1.13	0.22	−1.51
3	389 (31,569)	480 (2.58)	527	1.15	0.24	−1.43
4	398 (18,251)	496 (2.50)	484	0.91	0.0	−1.59

[a] Absorption peaks (λ_{max}) and molar extinction coefficients (ε) were measured in THF (2.2×10^{-5} M).
[b] Estimated from the onset of the absorption spectra in THF.
[c] Maximum λ of the fluorescence spectra in THF.
[d] The formal oxidation potentials (vs. NHE) in DCM containing 0.1 M of Bu_4NPF_6 as the supporting electrolyte with a scan rate of 100 mV/s and internally calibrated with ferrocene.
[e] Potential shift relative to dye **4.**
[f] The excited-state oxidation potential was calculated with the expression LUMO = HOMO − E_{0-0}.

M/cm at 541 nm for **N3**) [24] all the synthetized sensitizers show about ten times higher absorption coefficients, which allow the use of correspondingly thinner nanocrystalline films in the devices. This enhances electrolyte diffusion in the film and reduces the recombination of the light-induced charges during transportation [25]. The threshold absorption wavelengths of the absorption spectra for **1**, **2**, **3** and **4** are 507, 470, 480 and 496 nm, respectively, indicating that the absorption band for **1** is broader than the rest and results in a wide absorption in the longer wavelength region.

When dyes **1–4** are excited at their λ_{max} absorptions in an air-equilibrated solution at 298 K, they exhibit luminescence maxima at 456 (**2**), 466 (**4**), 526 (**3**) and 566 (**1**) nm. This indicates that the excited states of dyes **2–4** need more energy for the excitation than for **1**. The emission intensity reveals a more effective quenching process in dye **1**, which means that there is better coupling between the donor and acceptor moieties in this dye [30]. This suggests a better light harvesting ability of the solar spectrum for dye **1**.

Table 2
Absorption spectral data for the dyes in different solvents.

DYE	TOL λ_{max}/ nm	TOL+TEA λ_{max}/ nm	TOL+TFA λ_{max}/ nm	THF λ_{max}/ nm	THF+TEA λ_{max}/ nm	THF+TFA λ_{max}/ nm	DCM λ_{max}/ nm	DCM+TEA λ_{max}/ nm	DCM+TFA λ_{max}/ nm	EA λ_{max}/ nm	DMF λ_{max}/ nm
1	397	385	418	393	380	402	395	387	417	377	365
2	397	386	397	397	395	396	388	388	412	379	377
3	396	385	408	389	381	399	395	386	411	378	379
4	404	385	409	398	384	420	403	390	404	380	387

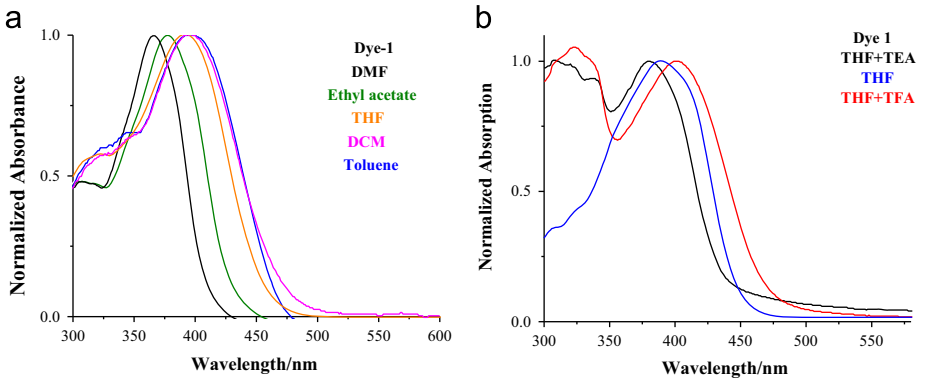

Fig. 3. Absorption spectra of **1** recorded in different solvents (a) and absorption spectra of **1** recorded in THF before and after the addition of TEA and TFA (b).

In general, all dyes showed negative solvatochromism of the higher wavelength absorption bands when recorded in solvents of different polarity, see Table 2 and Fig. 3. This is probably due to better solvation of the dyes in the polar solvents. This also confirms the charge transfer character for this electronic transition. Acid-base equilibria in solution could also change the donor–acceptor capabilities of the dyes. The existence of such equilibria was confirmed by the addition of trifluoroacetic acid (TFA) and triethylamine (TEA) to the dye solutions in toluene, DCM and THF, Table 2 and Fig. 3. Addition of TFA to the dye solutions resulted in a red-shift of the higher wavelength absorption because it shifts the equilibria to the acidic form. As expected, addition of TEA to the dye solutions results in notable blue shifts of the charge transfer transitions.

In order to determine the HOMO–LUMO levels and evaluate the possibility of electron transfer from the excited dye molecules to the conduction band of TiO_2 and regeneration by the electrolyte (I^-/I_3^-), the electrochemical properties of **1–4** were measured using cyclic voltammetry (CV) and differential pulse voltammetry (DPV) in DCM containing 0.1 M tetrabutylammonium hexafluorophosphate (Fig. 4). In all cases the first oxidation potential, which is attributed to oxidation of the triphenylamine group [31], is quasi-reversible, except for dye **1** which shows a reversible oxidation process. All first oxidation potential values fall between 0.9 and 1.18 V vs. NHE. On the other hand, **2** and **3** exhibit a second non-reversible oxidation potential at 1.53 and 1.71 V, respectively. A third non-reversible oxidation potential is observed at 1.71 V for **2**, which could be the result of oxidation of the bis(ethynylfluorene) π-spacer. Under similar conditions, **1** did not show a second oxidation within the measured electrochemical window. Finally, **4** exhibits a broad oxidation wave around 1.33 V, possibly corresponding to the second oxidation of the TPA core and/or oxidation of ($\equiv -Pt(PEt_3)_2 - \equiv$), as was reported previously for similar compounds [32]. The first oxidation potentials of these dyes shift to lower values upon changing the spacer from acetylene (**1**, 0.27 V) to the acetylide complex (**4**, 0.0 V) revealing that the electronic coupling between donor and acceptor groups notably decreases by changing the length, no matter the nature of the π-connection used.

The level of the highest occupied molecular orbital (HOMO) was estimated from the first oxidation wave relative to the NHE by addition of 0.63 V to the potentials measured vs. Fc/Fc^+, as listed in Table 1 [33]. The HOMO levels of all dyes were more positive than the reduction potential of the I^-/I_3^- pair (0.4 V vs. NHE) [34], ensuring sufficient driving force for the oxidized dyes to be reduced by the electrolyte. Meanwhile, the excited-state oxidation potential (E_{ox}^*) levels of the dyes were deduced from the first oxidation potential and the 0–0 transition energy (E_{0-0}) estimated from the edge of the absorption spectra. The (E_{ox}^*) level of all dyes was higher than the TiO_2 conductive band (−0.5 V vs. NHE) [34] thus ensuring the feasibility of electron injection, (Fig. 5).

2.3. Molecular orbital calculations

To understand the electronic structure of the dyes, their geometry was optimized by density functional theory (DFT) calculations at the 6-31G(d) or LanL2LZ level using the B3LYP functional, and the vertical excitation energies were computed using time-dependent density functional theory (TDDFT) by using the functional B3LYP or CAM-B3LYP in a vacuum and in THF solvent using the Gaussian 09 B.01 package.

The optimized molecular structures of **1–4** with different π-connectors are shown in Fig. 6. It is worth noting that the connectors do not have a significant influence on the torsion angle between the plane of the donor and that of the acceptor, which means that there is a high degree of π-conjugation that also suggests good electronic coupling between donor and acceptor moieties, which determines the charge transfer amplitude [13,35,36].

Electronic analyses show that the highest occupied molecular orbital (HOMO) is delocalized over the triphenylamine unit and the fluorene groups, except for **4,** for which it is located essentially

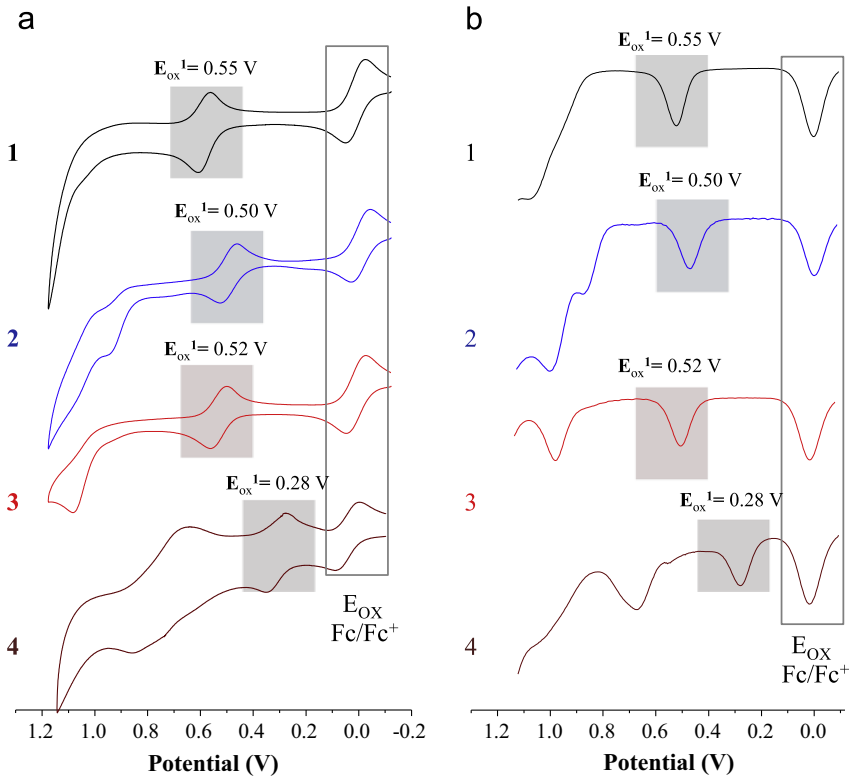

Fig. 4. Cyclic voltammograms (a) and differential pulse voltammograms (b) recorded in dichloromethane vs. Ferrocene/Ferrocenium (Fc/Fc^{+}) couple for the dyes **1–4**.

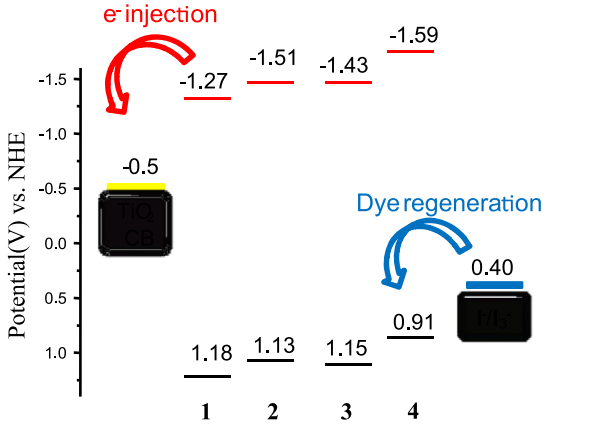

Fig. 5. Energy levels vs. NHE of **1–4** and of the other materials used for DSSC fabrication.

in the triphenylamine core. The LUMOs are mainly localized in the cyanoacrylic acid unit through the fluorenyl group (Table 3, Fig. 6). Thus the HOMO–LUMO excitation induced by irradiation could shift electron density from the triphenylamine to the cyano-acrylic acid group. This will ensure an efficient electron injection into the TiO_2 layer after light absorption by the sensitizer. Furthermore, comparison of the computed HOMO and LUMO energies with the edge of the CB of TiO_2 and the potential of the redox couple (Fig. 7) shows that they all have more negative HOMO energies than the I^{-}/I^{-3} redox couple (−4.8 eV vs. vacuum) [37], leading to a fast regeneration of the oxidized dyes. The more positive LUMO energies relative to the CB of TiO_2 (−4.0 eV vs. vacuum) [38] ensures an effective injection of excited electrons.

The longer wavelength transition calculated using B3LYP for the dyes are very red-shifted from the observed values in tetrahydrofuran and the vertical transitions calculated are predicted to originate exclusively from the HOMO/LUMO orbitals in all cases (Table 4). In contrast, the gas phase results obtained using the CAM-B3LYP functional show better agreement with the experimental data, with a slight blue shift observed if solvent effects are neglected. Solvent inclusion in the calculations of the vertical excitations using the PCM model show red shifts when compared with the experimentally observed values in tetrahydrofuran. The results obtained using different theories suggest significant contributions from HOMO/LUMO, HOMO−1/LUMO, HOMO/LUMO+1 transitions for these sensitizers. In particular, dyes **1** and **3** exhibit a high contribution from the HOMO/LUMO and a small contributions from the HOMO−1/LUMO transitions, while the maximum absorptions in **2** and **4** are governed mainly by HOMO−1/LUMO and HOMO/LUMO+1 transitions, with a slight contribution from the HOMO/LUMO transitions. On this basis, it can be argued that the longer wavelength absorptions result from charge transfer processes for **1** and **3**, and from π to π^{*} transitions for **2** and **4** [19,33].

2.4. Dye-sensitized solar cell (DSSC)

To prepare and study the DSSC, the doctor blading method was employed. After making the films they were annealed at 450 °C for 30 min. For sensitization, the films were impregnated with 0.5 mM of dyes **1–4** in THF for 24 h at room temperature. The samples were then rinsed with the same solvent to remove the excess of the dyes on the surface of the photo-electrodes and were air dried at room temperature. This was followed by addition of the redox electrolyte and the top contact of Pt coated FTO as discussed elsewhere. *J–V* characteristics were measured using a solar simulator at 100 mW/cm^2.

2.5. Photovoltaic measurements

Fig. 8 shows the photocurrent density–voltage (*J–V*) curves for all the devices under a simulated AM 1.5 solar irradiance at 100 mW/cm^2. Table 4 shows the measured photovoltaic parameters of the

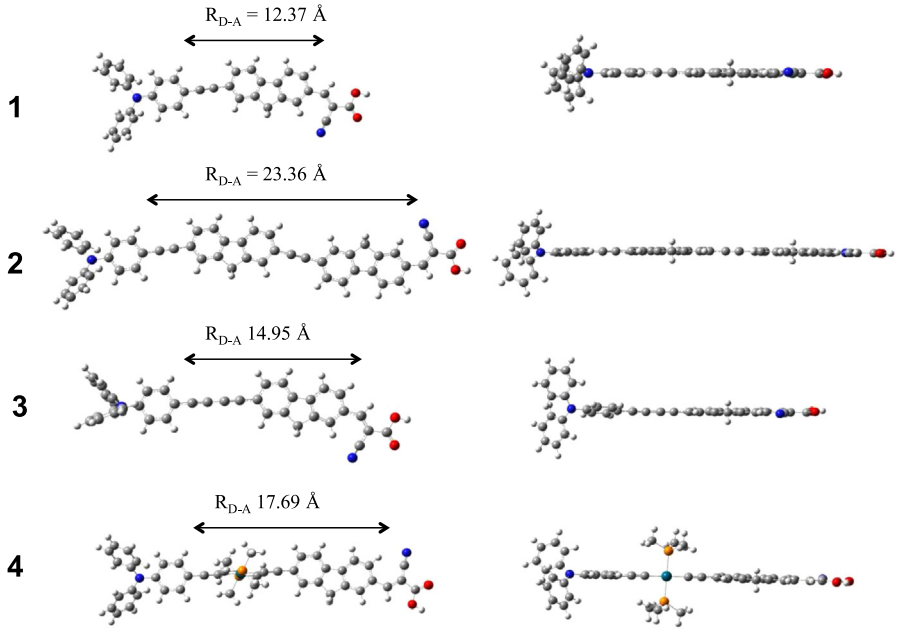

Fig. 6. Optimized molecular structures of dyes **1–4** in the gas phase, where R_{D-A} is the distance between donor and acceptor.

Table 3
Computed vertical transition energies, their oscillator strengths and configurations for the dyes **1–4** using different functionals.

Functional	Parameter	1	2	3	4
B3LYP (Vac)	λ_{max} (nm)	564	601	579	634
	F	0.8332	0.3725	0.6961	0.2017
	Configuration (contribution)	HOMO→LUMO (0.71)	HOMO→LUMO (0.70)	HOMO→LUMO (0.70)	HOMO→LUMO (0.71)
CAM-B3LYP (THF)	λ_{max} (nm)	410	400	401	412
	F	2.2929	3.7304	2.5918	1.9444
	Configuration (contribution)	HOMO→LUMO (0.56)	HOMO→LUMO (0.28)	HOMO→LUMO (0.42)	HOMO→LUMO (0.11)
		HOMO−1→LUMO (0.30)	HOMO−1→LUMO (0.46)	HOMO→LUMO+1 (0.27)	HOMO−1→LUMO (0.64)
CAM-B3LYP (Vac)	λ_{max} (nm)	398	392	393	392
	F	2.1213	3.6701	2.3503	1.1300
	Configuration (contribution)	HOMO→LUMO (0.57)	HOMO→LUMO (0.30)	HOMO→LUMO (0.44)	HOMO→LUMO (0.15)
		HOMO−1→LUMO (0.28)	HOMO→LUMO+1 (0.42)	HOMO−1→LUMO (0.29)	HOMO−1→LUMO (0.70)
	HOMO (eV)	−6.09	−6.19	−6.41	−6.32
	LUMO (eV)	−1.56	−1.71	−1.76	−1.90

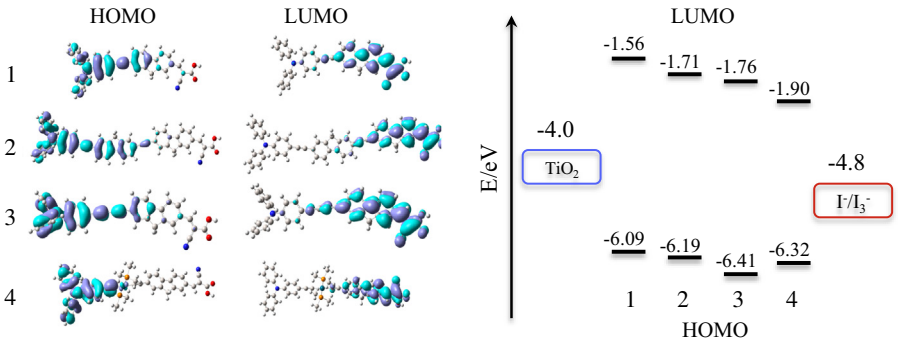

Fig. 7. Frontier orbitals of sensitizers **1–4** optimized with DFT at the CAM-B3LYP/6-31G(d) level in vacuum.

DSSCs of the four dyes. The concentration of all four dyes was the same, i.e. 0.5 mM. Commercially available Degussa (P25) was used for making the photo-anodes. Films were dipped in all the respective dyes for 24 h. The **1** gives the highest efficiency, 3.50%, compared to all other dyes. All these dyes show very similar open circuit voltage V_{oc} values, but the current density J_{sc} for **1** is higher, 7.78 mA/cm^2, than for all other dyes as a result of its broader absorption spectrum, which is the main reason for its higher photo-conversion efficiency.

These photovoltaic performances are in agreement with the theoretical, optical and electrochemical studies that predict a better performance for the shortest linkage. The four compounds synthesized show optical and electrochemical properties that are consistent with the distance between donor and acceptor groups. The transition bands show a more pronounced intramolecular charge transfer (ICT) character for shorter linkages [**1** (R_{D-A}=12.47 Å) > **3** (R_{D-A}=14.95 Å) > **4** (R_{D-A}=17.69 Å) > **2** (R_{D-A}=23.36 Å)], which

Table 4
Performance parameters of DSSCs fabricated with dyes **1–4**.

Dye	V_{oc} (V)	J_{sc} (mA/cm^2)	FF (%)	PCE (%)
1	0.680	7.78	66.00	3.50
2	0.670	4.35	62.00	1.80
3	0.630	6.05	66.00	2.52
4	0.650	4.50	70.00	2.00

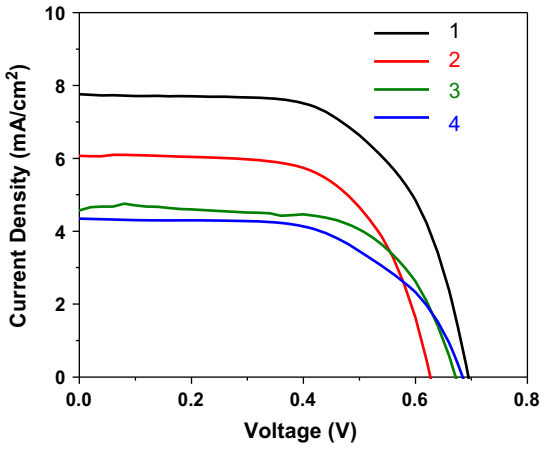

Fig. 8. Solar cell characteristics for the case of four different dyes **1–4**.

follows the same tendency observed for the oxidation peak shifts [**1** (0.27 V) > **3** (0.24) > **2** (0.22) > **4** (0.0)]. Therefore, the introduction of additional acetylene conjugation linkages in these kinds of pigments decreases the donor–acceptor interactions and subsequently leads to lower photovoltaic performances.

3. Conclusions

We have successfully synthesized a series of new dyes, **1–4,** based on triphenylamine, fluorene and cyanoacrylic acid using different acetylene linkages, acetylene (**1**), 2,7-bisethynylfluorene (**2**), 1,4-butynyl (**3**) and a *trans*-platinum acetylide (**4**). Both theoretical and experimental results show that there is sufficient thermodynamic driving force to inject electrons from the dyes to the conduction band of TiO_2 and for electron injection from the redox electrolyte to the sensitizers. These results clearly demonstrate that the introduction of acetylene π-bridges into TPA-fluorene sensitizers can obviously extend the conjugated system and enhance the molar extinction coefficient. Unexpectedly, we found that the DSSC performance of these dyes decreases as the π-bridge length is increased, which is probably due to the presence of elongated conjugation pathways, which minimizes the donor–acceptor interaction and produces a higher energy optical excitation.

Based on these results, additional work is currently focused on developing improved absorption properties by changing the acceptor moiety in dye **1**. Additionally, we are working on designing and synthesizing dyes that inhibit aggregation and recombination processes by introducing highly hindered groups in the donors.

Acknowledgements

The authors gratefully acknowledge financial support from COLCIENCIAS and Universidad del Valle. Luis Echegoyen wishes to thank the US National Science Foundation, grants DMR-1205302 (PREM Program) and the Airforce Office of Scientific Research (grants FA9550-12-1-0053 and FA9550-12-1-0468) for generous financial support. Luis Echegoyen also wishes to thank the Robert A. Welch Foundation for an endowed chair, grant # AH-0033, for generous support. Nazario Martín thanks to the MINECO of Spain (Project CTQ2011-24652) for financial support.

Appendix A. Supporting information

Supplementary data associated with this article can be found in the online version at http://dx.doi.org/10.1016/j.solmat.2013.10.035.

References

[1] M. Grätzel, Recent advances in sensitized mesoscopic solar cells, Acc. Chem. Res. 42 (2009) 1788–1798.
[2] B. O'Regan, M. Grätzel, A low-cost, high-efficiency solar cell based on dye-sensitized colloidal TiO_2 films, Nature 353 (1991) 737–740.
[3] A. Hagfeldt, G. Boschloo, L. Sun, L. Kloo, H. Pettersson, Dye-sensitized solar cells, Chem. Rev. 110 (2010) 6595–6663.
[4] F.d.r. Labat, T. Le Bahers, I. Ciofini, C. Adamo, First-principles modeling of dye-sensitized solar cells: challenges and perspectives, Acc. Chem. Res. 45 (2012) 1268–1277.
[5] T. Funaki, H. Funakoshi, O. Kitao, N. Onozawa-Komatsuzaki, K. Kasuga, K. Sayama, H. Sugihara, Cyclometalated ruthenium(II) complexes as near-IR sensitizers for high efficiency dye-sensitized solar cells, Angew. Chem. Int. Ed. 51 (2012) 7528–7531.
[6] Z. Ning, H. Tian, Triarylamine: a promising core unit for efficient photovoltaic materials, Chem. Commun. (2009) 5483–5495.
[7] J.-H. Yum, P. Walter, S. Huber, D. Rentsch, T. Geiger, F. Nuesch, F. De Angelis, M. Grätzel, M.K. Nazeeruddin, Efficient far red sensitization of nanocrystalline TiO_2 films by an unsymmetrical squaraine dye, J. Am. Chem. Soc. 129 (2007) 10320–10321.
[8] T.-H. Kwon, V. Armel, A. Nattestad, D.R. MacFarlane, U. Bach, S.J. Lind, K.C. Gordon, W. Tang, D.J. Jones, A.B. Holmes, Dithienothiophene (DTT)-based dyes for dye-sensitized solar cells: synthesis of 2,6-dibromo-DTT, J. Org. Chem. 76 (2011) 4088–4093.
[9] K. Guo, K. Yan, X. Lu, Y. Qiu, Z. Liu, J. Sun, F. Yan, W. Guo, S. Yang, Dithiafulvenyl unit as a new donor for high-efficiency dye-sensitized solar cells: synthesis and demonstration of a family of metal-free organic sensitizers, Org. Lett. 14 (2012) 2214–2217.
[10] H. Imahori, T. Umeyama, S. Ito, Large œÄ-Aromatic molecules as potential sensitizers for highly efficient dye-sensitized solar cells, Acc. Chem. Res. 42 (2009) 1809–1818.
[11] A. Yella, H.-W. Lee, H.N. Tsao, C. Yi, A.K. Chandiran, M.K. Nazeeruddin, E.W.-G. Diau, C.-Y. Yeh, S.M. Zakeeruddin, M. Grätzel, Porphyrin-sensitized solar cells with cobalt (II/III) based redox electrolyte exceed 12 percent efficiency, Science 334 (2011) 629–634.
[12] S. Wenger, P.-A. Bouit, Q. Chen, J.l. Teuscher, D.D. Censo, R. Humphry-Baker, J.-E. Moser, J.L. Delgado, N. Marín, S.M. Zakeeruddin, M. Grätzel, Efficient electron transfer and sensitizer regeneration in stable π-extended tetrathiafulvalene-sensitized solar cells, J. Am. Chem. Soc. 132 (2010) 5164–5169.
[13] J. Zhang, H.-B. Li, S.-L. Sun, Y. Geng, Y. Wu, Z.-M. Su, Density functional theory characterization and design of high-performance diarylamine-fluorene dyes with different π spacers for dye-sensitized solar cells, J. Mater. Chem. 22 (2012) 568–576.
[14] A. Baheti, P. Singh, C.-P. Lee, K.R.J. Thomas, K.-C. Ho, 2,7-Diaminofluorene-based organic dyes for dye-sensitized solar cells: effect of auxiliary donor on optical and electrochemical properties, J. Org. Chem. 76 (2011) 4910–4920.
[15] M.S. Khan, M.R.A. Al-Mandhary, M.K. Al-Suti, B. Ahrens, M.F. Mahon, L. Male, P.R. Raithby, C.E. Boothby, A. Kohler, Synthesis, characterisation and optical spectroscopy of diynes and poly-ynes containing derivatised fluorenes in the backbone, Dalton Trans. (2003) 74–84.
[16] M. Wielopolski, J. Santos, B.M. Illescas, A. Ortiz, B. Insuasty, T. Bauer, T. Clark, D.M. Guldi, N. Martin, Vinyl spacers-tuning electron transfer through fluorene-based molecular wires, Energy Environ. Sci. 4 (2011) 765–771.
[17] O. Ingañas, F. Zhang, M.R. Andersson, Alternating polyfluorenes collect solar light in polymer photovoltaics, Acc. Chem. Res. 42 (2009) 1731–1739.
[18] C.-H. Wu, T.-Y. Pan, S.-H. Hong, C.-L. Wang, H.-H. Kuo, Y.-Y. Chu, E.W.-G. Diau, C.-Y. Lin, A fluorene-modified porphyrin for efficient dye-sensitized solar cells, Chem. Commun. 48 (2012) 4329–4331.
[19] P. Shen, Y. Tang, S. Jiang, H. Chen, X. Zheng, X. Wang, B. Zhao, S. Tan, Efficient triphenylamine-based dyes featuring dual-role carbazole, fluorene and spirobifluorene moieties, Org. Electron. 12 (2011) 125–135.
[20] H. Choi, C. Baik, S.O. Kang, J. Ko, M.-S. Kang, M.K. Nazeeruddin, M. Grätzel, Highly efficient and thermally stable organic sensitizers for solvent-free dye-sensitized solar cells, Angew. Chem. Int. Ed. 47 (2008) 327–330.

[21] S. Kim, J.K. Lee, S.O. Kang, J. Ko, J.H. Yum, S. Fantacci, F. De Angelis, D. Di Censo, M.K. Nazeeruddin, M. Grätzel, Molecular engineering of organic sensitizers for solar cell applications, J. Am. Chem. Soc. 128 (2006) 16701–16707.
[22] A.M.Fabio Silvestri, Acetylene-based materials in organic photovoltaics, Int. J. Mol. Sci. 11 (2010) 1471–1508.
[23] Y.-D. Lin, T.J. Chow, Geometrical effect of stilbene on the performance of organic dye-sensitized solar cells, J. Mater. Chem. 21 (2011) 14907–14916.
[24] W. Wu, X. Xu, H. Yang, J. Hua, X. Zhang, L. Zhang, Y. Long, H. Tian, D-π-M-π-A structured platinum acetylide sensitizer for dye-sensitized solar cells, J. Mater. Chem. 21 (2011) 10666–10671.
[25] W. Wu, J. Zhang, H. Yang, B. Jin, Y. Hu, J. Hua, C. Jing, Y. Long, H. Tian, Narrowing band gap of platinum acetylide dye-sensitized solar cell sensitizers with thiophene π-bridges, J. Mater. Chem. 22 (2012) 5382–5389.
[26] X. Zhao, C. Piliego, B. Kim, D.A. Poulsen, B. Ma, D.A. Unruh, J.M.J. Frechet, Solution-processable crystalline platinum-acetylide oligomers with broad-band absorption for photovoltaic cells, Chem. Mater. 22 (2010) 2325–2332.
[27] W. Lu, B.-X. Mi, M.C.W. Chan, Z. Hui, C.-M. Che, N. Zhu, S.-T. Lee, Light-emitting tridentate cyclometalated platinum(II) complexes containing σ-alkynyl auxiliaries: tuning of photo- and electrophosphorescence, J. Am. Chem. Soc. 126 (2004) 4958–4971.
[28] C.A. Echeverry, A. Tigreros, A. Ortiz, B. Insuasty, N. Martín, Free-base tetraarylporphyrin covalently linked to [60]fullerene through ethynylfluorene spacer, J. Porphyrins Phthalocyanines 15 (2011) 1231–1238.
[29] N. He, B. Li, H. Zhang, J. Hua, S. Jiang, Synthesis, two-photon absorption and optical limiting properties of new linear and multi-branched bithiazole-based derivatives, Synth. Met. 162 (2012) 217–224.
[30] M. Wielopolski, G. de Miguel Rojas, C. van der Pol, L. Brinkhaus, G. Katsukis, M. R. Bryce, T. Clark, D.M. Guldi, Control over charge transfer through molecular wires by temperature and chemical structure modifications, ACS Nano 4 (2010) 6449–6462.
[31] K. Onitsuka, N. Ohara, F. Takei, S. Takahashi, Synthesis and redox properties of trinuclear ruthenium-acetylide complexes with tri(ethynylphenyl)amine bridge, Dalton Trans. (2006) 3693–3698.
[32] C. Liao, J.E. Yarnell, K.D. Glusac, K.S. Schanze, Photoinduced charge separation in platinum acetylide oligomers, Ä†, J. Phys. Chem. B 114 (2010) 14763–14771.
[33] P. Singh, A. Baheti, K.R.J. Thomas, C.-P. Lee, K.-C. Ho, Fluorene-based organic dyes containing acetylene linkage for dye-sensitized solar cells, Dyes Pigm. 95 (2012) 523–533.
[34] X. Cheng, S. Sun, M. Liang, Y. Shi, Z. Sun, S. Xue, Organic dyes incorporating the cyclopentadithiophene moiety for efficient dye-sensitized solar cells, Dyes Pigm. 92 (2012) 1292–1299.
[35] H. Tan, C. Pan, G. Wang, Y. Wu, Y. Zhang, G. Yu, M. Zhang, A comparative study on properties of two phenoxazine-based dyes for dye-sensitized solar cells, Dyes Pigm. 101 (2014) 67–73.
[36] Z. Wan, C. Jia, L. Zhou, W. Huo, X. Yao, Y. Shi, Influence of different arylamine electron donors in organic sensitizers for dye-sensitized solar cells, Dyes Pigm. 95 (2012) 41–46.
[37] A. Hagfeldt, M. Graetzel, Light-induced redox reactions in nanocrystalline systems, Chem. Rev. 95 (1995) 49–68.
[38] J.B. Asbury, Y.-Q. Wang, E. Hao, H.N. Ghosh, T. Lian, Evidences of hot excited state electron injection from sensitizer molecules to TiO_2 nanocrystalline thin films, Res. Chem. Intermed. 27 (2001) 393–406.